Journal of *Marine Science and Engineering*

MDPI

Article

A Global-Ocean-Data Assimilation for Operational Oceanography

Yinghao Qin [1,2], Qinglong Yu [1,2,*], Liying Wan [1,2,*], Yang Liu [1,2], Huier Mo [1,2], Yi Wang [1,2], Sujing Meng [1,2], Xiangyu Wu [1,2], Dandan Sui [3] and Jiping Xie [4]

[1] National Marine Environmental Forecasting Center (NMEFC), Beijing 100081, China; qinyh@nmefc.cn (Y.Q.); liuyang@nmefc.cn (Y.L.); huier.mo@nmefc.cn (H.M.); wangyi@nmefc.cn (Y.W.); mengsujing@163.com (S.M.); wxy@nmefc.cn (X.W.)
[2] Key Laboratory of Marine Hazards Forecasting, National Marine Environmental Forecasting Center, Beijing 100081, China
[3] South China Sea Institute of Oceanology (SCSIO), Chinese Academy of Sciences (CAS), Guangzhou 510301, China; sui@scsio.ac.cn
[4] Nansen Environmental and Remote Sensing Center (NERSC), 5007 Bergen, Norway; jiping.xie@nersc.no
* Correspondence: yuql@nmefc.cn (Q.Y.); liying.wan@nmefc.cn (L.W.)

Abstract: In this study, a global-ocean-data-assimilation system based on the three-dimensional variational (3DVAR) scheme is built for operational oceanography. The available observations include satellite altimetry; the satellite-measured sea-surface temperature (SST); and T/S profiles from Argo floats, which are assimilated to provide the initial condition of the global-ocean forecasting. The statistical analysis methods are designed to assess the performance of the data-assimilation scheme, and the results show that the analysis SST fields agree well with OSTIA and MGDSST, and the corresponding root-mean-square errors are, respectively, 0.523 and 0.548 °C. Moreover, the analysis sea-surface-height fields are well represented at the middle and low latitudes and have a slightly greater difference in the regions with strong mesoscale eddies. The variations in the vertical distribution of the forecasting temperature profiles resemble those of the GTS buoy observation. The forecasting salinity profiles correspond well to GTS observations, except with a weaker cold bias between the depths 100 and 200 m (about 0.2 PSU) at buoy station 2901494. Overall, our 3DVAR assimilation system plays a significant role in improving the accuracy of analysis and forecasting fields for operational oceanography.

Keywords: data assimilation; 3DVAR; operational oceanography; ocean forecasting; satellite remote; statistical analysis

Citation: Qin, Y.; Yu, Q.; Wan, L.; Liu, Y.; Mo, H.; Wang, Y.; Meng, S.; Wu, X.; Sui, D.; Xie, J. A Global-Ocean-Data Assimilation for Operational Oceanography. *J. Mar. Sci. Eng.* **2023**, *11*, 2255. https://doi.org/10.3390/jmse11122255

Academic Editor: João Miguel Dias

Received: 2 October 2023
Revised: 6 November 2023
Accepted: 24 November 2023
Published: 29 November 2023

1. Introduction

The marine-surface environment, which accounts for approximately 71% of the Earth's surface, is significant for air–sea interactions. Due to the high specific heat capacity of ocean water, the global ocean plays a major role in global climate change, especially in extreme weather and climate events, which have wide impacts on people's lives and the social economy [1]. Global-ocean numerical forecasting and climate-change projections can provide important guidance for our administrative management.

The marine economy has gradually grown since the beginning of the twenty-first century, and this has played an indispensable role in economic development. With the rapid development of the marine economy, we must attach great importance to global-ocean forecasting and support for major events, such as the exploitation and utilization of deep-ocean resources, global shipping services, marine fisheries, the construction of submarine oil pipelines and search and rescue. To ensure the marine safety of transport channels, it is necessary to provide marine-environment forecasting from near-shore and coastal areas to the global oceans. For this reason, building a global-ocean-circulation numerical

forecasting system is of great significance for promoting the sustainable development of the marine economy.

Ocean-data assimilation can effectively combine multisource observation information with ocean numerical simulation and provide the optimal estimation of the ocean state at a given time. As the initial condition for ocean forecasting, ocean-data assimilation is an important guarantee for improving the ability of marine-environmental forecasting by reducing the uncertainty of the initial values [2].

Global-ocean-circulation numerical forecasting systems have been built by many countries throughout the world. For example, the US Navy's operational numerical forecasting system for global oceans was developed with the Hybrid Coordinate Ocean Model (HYCOM) and the Navy-Coupled Ocean-Data Assimilation (NCODA) [3–5]. The Forecast Ocean-Assimilation Model (FOAM) [6], which comprises the Nucleus for European Modeling of the Ocean (NEMO) and Louvain-la-Neuve sea-ice model (LIM), is an operational global-ocean forecasting system created by the UK Met Office, who also developed the 3DVAR method NEMOVAR to replace the analysis-correction scheme [7–11]. Mercator Ocean also designed the second-generation Mercator Assimilation Suite (SAM2) [12,13], based on the Singular Extended Evolutive Kalman (SEEK) filtering-analysis method [14,15], to provide the initial conditions for global-ocean forecasting [16–18]. China's National Marine Environmental Forecasting Center (NMEFC) built the Chinese Global Operational Oceanography Forecasting System, which includes the global-ocean circulation numerical forecasting subsystem based on the Modular Ocean Model (MOM.v4) [19], NMEFC-MOM4; the global-sea-surface-wind numerical forecasting subsystem, NMEFC-WIND; the global-wave numerical forecasting subsystem based on WAVEWATCH III (v3.14) [20], NMEFC-NWW3; and the global-tide-and-tidal-current numerical forecasting subsystem by using the Finite-Volume Coastal Ocean Model (FVCOM) [21], NMEFC-FVCOM. NMEFC-WIND is composed of five different segments: a data-download module, Grid-point Statistical Interpolation (GSI) [22,23] module for data assimilation, Global Spectral Model (GSM) [24] module for forecasting, postprocessing module and product-evaluation module. The horizontal resolution of NMEFC-WIND is T382 (about 34 km). The data-assimilation module (GSI) is run four times per day at 18:00, 00:00, 06:00 and 12:00. Next, the forecasting module (GSM) is started once a day at 12:00, with the initial conditions provided by the GSI and provides 168 h sea-surface-wind forecasting. The horizontal resolution of NMEFC-FVCOM is 0.06~2.0° with 40 vertical levels. The topography is obtained from the Digital Bathymetric Data Base 5 (DBDB5) and 2 min gridded global relief data (ETOPO2). The nudging scheme is adopted by assimilating the Integrated Geophysical Data Record (MGDR) and Geophysical Data Record (GDR) from the French Space Agency CNES with the Jet Propulsion Laboratory (JPL), California Institute of Technology (Caltech or CIT). NMEFC-FVCOM is run once a day to provide tidal-current and water-level forecasting. NMEFC-MOM4 uses the 3DVAR method to assimilate the remote-sensing-measured sea-surface temperature, Merged Sea-Level Anomaly (MSLA) from AVISO and salinity and temperature profiles obtained from Argo floats. NMEFC-MOM4 can operationally provide full-range real-time ocean-environmental-forecasting services for marine-disaster prevention and reduction, marine search and rescue and oil spills, maintaining marine rights and interests, safe sailing and responding to major emergency events.

In this paper, we give a detailed introduction to this global-ocean data-assimilation system for operational oceanography and examine the performance of NMEFC-MOM4. To do so, we evaluate different aspects of the ocean fields of NMEFC-MOM4 by comparing them with the corresponding observation datasets. The remainder of this study is organized as follows. In Section 2, we give a brief description of the ocean model and its assimilation scheme, along with the datasets employed in this paper. Section 3 presents the main results of the performance evaluation of the NMEFC-MOM4 forecasting system. Finally, Section 4 provides the study's summary and conclusions.

2. Assimilation Scheme and Datasets

2.1. Ocean Model

The global-ocean forecasting system is built with MOM4. The model uses the explicit free-surface method to determine the vertical coordinate and B-grid to define the horizontal arrangement of the model fields. The model uses a global tripolar grid to avoid the singularity of the spherical coordinate at the geographical North Pole. The global horizontal resolution in the meridional and zonal direction is $1/4^\circ \times 1/4^\circ$. There are 50 vertical levels with about a 10 m resolution in the top-surface layers. The model's topography is OCCAM 2 arc minute. We employ the non-Boussinesq approach [25] rather than the traditional volume-conserving approach. Hence, the model's sea level can be simulated more accurately under the mass-conserving framework. For the physical parameterization schemes, the model uses the overflow algorithm of Campin and Goosse [26], McWilliams skew diffusivity [27], neutral tracer diffusion of Griffies et al. [28] and K-profile parameterization (KPP) [29] for vertical mixing simulation in the upper ocean. More details of MOM4 can be found in a technical guide at the NOAA's Geophysical Fluid Dynamics Laboratory (GFDL) [19].

2.2. Assimilation Scheme

The global-ocean forecasting system is a 3DVAR-employed assimilation scheme, and the control variables of 3DVAR's cost function are the salinity and temperature fields. The available assimilation observations include satellite altimetry, the satellite remote-sensing-measured SST and temperature–salinity profiles from Argo floats. For cases that are relevant to NMEFC-MOM4, the entire process of the 3DVAR assimilation scheme can be split into two steps. First, we can estimate the vertical temperature and salinity distribution by selecting the optimal solution of the following 3DVAR's cost function:

$$\begin{aligned} J &= J_b + J_o \\ J_b &= (t - t_b)^T B_{t1}^{-1}(t - t_b) + (s - s_b)^T B_{s1}^{-1}(s - s_b) \\ J_o &= (h(t,s) + h_c(t_s, s(t_b)) - h_m - h_o)^T R_1^{-1}(h(t,s) + h_c(t_s, s(t_b)) - h_m - h_o) \end{aligned} \tag{1}$$

where t and s are the analysis temperature and salinity control vectors, respectively; t_b and s_b denote the background information of the model simulation; B_{t1} and B_{s1} are the vertical background-error covariance matrices; R_1 is the error covariance matrix for observation; h_o is the sea-surface-height anomaly of the altimeter data; and h_m is the average sea-surface height of the model simulation. $h_c(t,s) = -\int_0^{z_m} \frac{\rho(t,s,p)-\rho_r(p)}{\rho_r(p)} dz$ is calculated by projecting observations of the SST downward. Here, $\rho(t,s,p)$ is the seawater density; $\rho_r(p) = \rho(0, 35, p)$ is the reference ocean density and $z_m = 1000$ m is the reference constant depth. In this way, the SST and SSH can be assimilated simultaneously as one control variable, avoiding the definition of their respective observations' error covariance matrices.

Next, the cost function at every model horizontal level can be defined by using the pseudo-observation vectors, which are the temperature and salinity obtained in the first step:

$$\begin{aligned} J &= J_b + J_o \\ J_b &= (t - t_b)^T B_{t2}^{-1}(t - t_b) + (s - s_b)^T B_{s2}^{-1}(s - s_b) \\ J_o &= (Ht - t_o)^T R_t^{-1}(Ht - t_o) + (Hs - s_o)^T R_s^{-1}(Hs - s_o) \end{aligned} \tag{2}$$

where B_{t2} and B_{s2} are the horizontal backgrounds of the temperature and salinity fields, respectively; R_t and R_s are the observation error covariance matrices; subscripts t and s represent the temperature and salinity fields, respectively; and H is the observational operator. We assume that the measurement errors are uncorrected so that the observation error covariance matrices are diagonal. The temperature and salinity observations' error

covariances are set to 0.1 and 0.05, respectively. The background-error covariance matrices are defined in the form of a Gaussian function:

$$B = A\exp\left(-\frac{\Delta x^2}{L_x^2} - \frac{\Delta y^2}{L_y^2}\right) \quad (3)$$

The different correlation scales are given in the meridional and latitudinal directions. Here, we empirically set $L_x = 450$ km, $L_y = 650$ km for the temperature and $L_x = 420$ km, $L_y = 510$ km for the salinity; Δx and Δy are the east–west and south–north distances for any two grid points; and A is the background-error variance, which is set to 2.0 for temperature and 0.15 for salinity. For a detailed description and additional information on the assimilation scheme, please refer to the associated published articles [30,31].

This global-ocean forecasting system was put into operational forecasting at the National Marine Environmental Forecasting Center in March 2013 and has since been run daily with the Global Forecasting System (GFS) atmospheric forcing fields from the National Centers for Environmental Prediction (NCEP). The NMEFC-MOM4 can provide a wide variety of forecasting products including sea temperature, salinity, current, ocean mixed-layer depth and sea-surface height (Figure 1). All the operational global-ocean-forecasting products are made available online through the NMEFC home page (https://www.nmefc.cn/). For special requirements, we can also customize products according to user needs. The corresponding products can be released by television, radio and other common platforms that users follow.

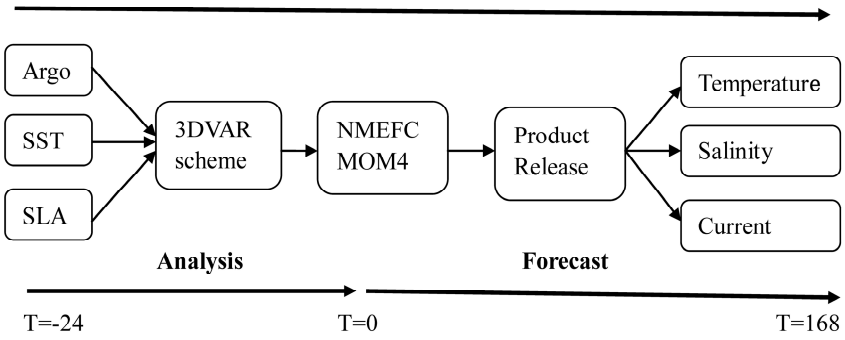

Figure 1. Schematic diagram of the global-ocean-circulation operational numerical forecasting system (NMEFC-MOM4).

2.3. Datasets

For the assimilation observations in NMEFC-MOM4, satellite remote sensing of the real-time, global, sea-surface temperature (RTG SST) was downloaded from ftp://ftpprd.ncep.noaa.gov (accessed on 1 March 2013). The sea-surface altimeter datasets were sourced from the Archiving, Validation and Interpretation of Satellite Oceanographic (AVISO) data of the French Space Agency (CNES). The satellite observations with depths shallower than 200 m are masked and then thinned to regular coarse-grid subsets in the assimilation. It should be noted that the objective analysis products of satellite remote sensing are not perfect. They are pragmatic references with some limitations in the ocean-data assimilation [32], especially in the operational forecasting systems [33–35]. The temperature–salinity profiles from Argo floats can be obtained from the network through the FTP site ftp://ftp.ifremer.fr/ifremer/argo (accessed on 27 February 2013). These Argo profile observations themselves contain different quality-control-flag (1–9) information. The flag = 1 indicates that the profiles contain good data, which pass all real-time quality-control automatic tests. The missing values are flagged with code 9. There is also an important value, DATA_MODE, in the profile descriptions. If DATA_MODE is 'R', there are no adjusted data. If DATA_MODE is 'D' or 'A', there are adjusted data. Therefore, we firstly choose good data with a quality flag = 1 for the temperature, salinity and pressure. Secondly, we replace

these three variables with the corresponding adjusted values only if the DATA_MODE is 'D' or 'A'. Additionally, an additional quality control measure is employed to arrange the profiles from lower to higher values of the pressure at the vertical level.

For the verification of NMEFC-MOM4, we used the Operational Sea-Surface Temperature and Ice Analysis (OSTIA) from https://marine.copernicus.eu/ (accessed on 2 August 2013) and the Merged satellite and Global Daily SST (MGDSST) in situ data from the Japan Meteorological Agency (JMA). The OSTIA, which has a special resolution of $1/20^{\circ}$, was formed by combining EnviSat/AATSR, Aqua/AMSR-E, NOAA/AVHRR, DMSP/SSMI/I, MSG1/SEVIRI, TRMM/TMI and the in situ temperature and salinity [36]. The MGDSST is available at a $1/4^{\circ} \times 1/4^{\circ}$ resolution and is daily averaged by merging the remote satellite of AMSR-E and NOAA/AVHRR and the in situ observations with three-dimensional optimum interpolation (OI) methods [37]. The Global Telecommunication System (GTS) buoy data were also used for a point-by-point evaluation of the temperature and salinity profiles.

2.4. Evaluation Method

To quantitatively evaluate the performance of NMEFC-MOM4, we use statistics to better describe the accuracy by comparing with the observations, including the model bias and root-mean-square error (RMSE). At the same time, we use the standard deviation (STD) to estimate the measure of the variability of the ocean-forecasting and analysis fields. These formulas are as follows:

$$\mathrm{Bias}(x,y) = \frac{1}{T}\sum_{t=1}^{T}\left(\mathrm{M}(x,y,t) - O(x,y,t)\right) \tag{4}$$

$$\mathrm{RMSE}(x,y) = \sqrt{\frac{1}{T}\sum_{t=1}^{T}\left(\mathrm{M}(x,y,t) - O(x,y,t)\right)^2} \tag{5}$$

$$\mathrm{STD}(x,y) = \sqrt{\frac{1}{T}\sum_{t=1}^{T}\left(\mathrm{M}(x,y,t) - \overline{\mathrm{M}}(x,y)\right)^2} \tag{6}$$

where x, y, t are the longitude, latitude and time dimension, respectively; $\mathrm{M}(x,y,t)$ $O(x,y,t)$ is the numerical simulation or forecasting and observations at (x,y,t), respectively; T represents the total number of elements along the time-of-day dimension; and $\overline{\mathrm{M}}(x,y)$ denotes the mean value for the elements along the dimension of the time of day.

3. Results

Evaluation is important and necessary for ocean-data-assimilation and forecasting systems. We evaluate and validate forecasting products with many kinds of observations by focusing on their statistical and physical properties. Since the NMEFC-MOM4 Global Forecasting System has assimilated the satellite altimetry, sea-surface temperature and Argo temperature–salinity profiles in analysis fields, it is highly necessary and important to assess their prediction accuracy. For this reason, we will evaluate the performance of data assimilation on the sea-surface temperature in terms of the model bias and root-mean-square error, and then we plan to assess the sea-surface height.

3.1. Analysis-Error Statistics of SST

In this section, to assess the analysis fields of the SST from NMEFC-MOM4, we compare them with the OSTIA and MGDSST. The SST average differences from March to July 2013 between NMEFC-MOM4 and these two kinds of observations are shown in Figure 2.

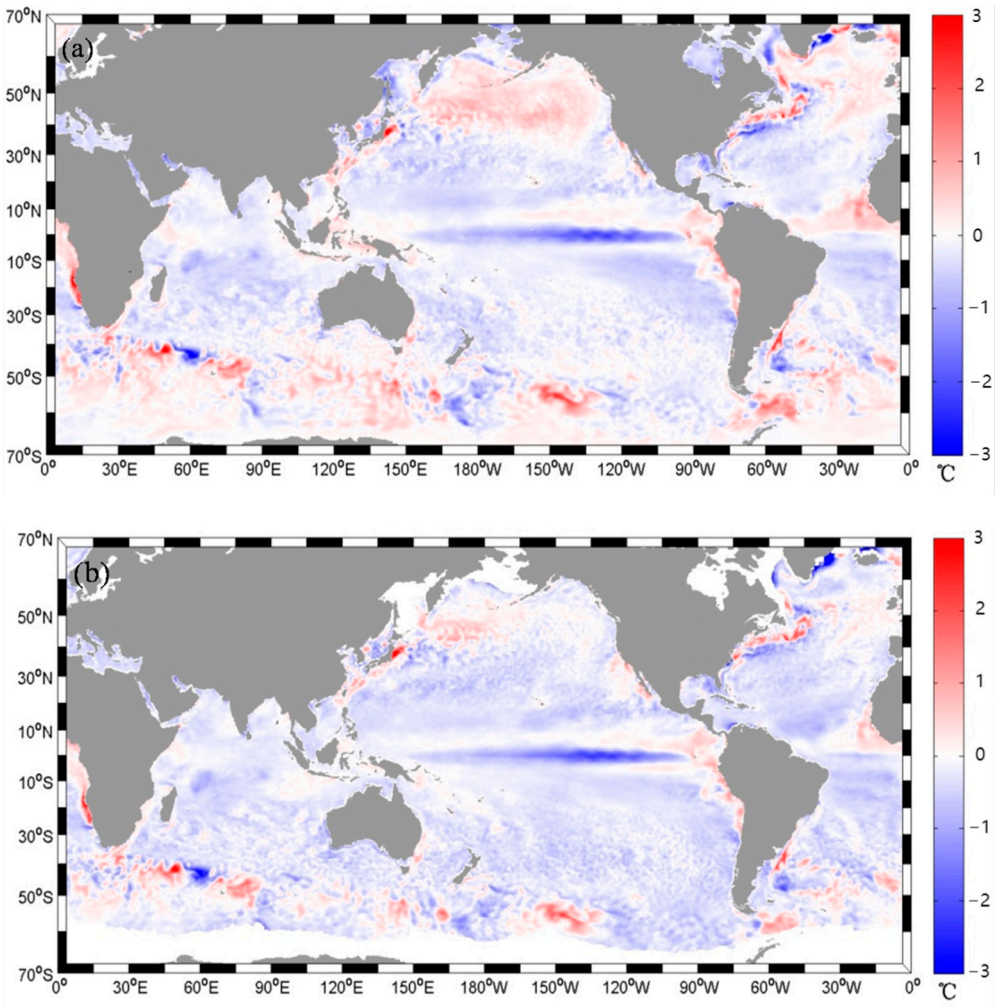

Figure 2. Distributions of global SST bias (°C) against the (**a**) OSTIA and (**b**) MGDSST.

The analysis SST of NMEFC-MOM4 is, overall, in good agreement with the observations. The model biases calculated from the two kinds of sea-surface-temperature data have a similar pattern of spatial distribution. In these regions with intense mesoscale activity and strong SST gradients, such as the Kuroshio extension, Gulf Stream and several regions in middle and high latitudes, the analysis SST tends to be overestimated in comparison with the OSTIA and MGDSS. In addition, the high and low values are alternately distributed in the West Wind Drift (WWD) region. The analysis SST is basically underestimated in the tropical regions, particularly over the Tropical Eastern Pacific, which may be due to the relative strong mixing parameterization of the dynamical process. The air–sea interaction is active, and the thermocline structure is sensitive to wind forcing in this region [38]. McClean et al. [39] and Delworth et al. [40] revealed that a higher-resolution ocean model can improve the SST bias in the equatorial and Eastern Pacific. The global model bias between the analysis SST and OSTIA (about −0.085 °C) is much closer to zero than that obtained from the MGDSST datasets (about −0.225 °C).

Next, we analyze the spatial distribution of the RMSE for the analysis SST relative to the OSTIA and MGDSST (Figure 3). The overall spatial average RMSE values calculated from the OSTIA and MGDSST are 0.523 and 0.548 °C, respectively. It should be noted that higher RMSE values often occur in regions characterized by relatively high SST average differences. Similarly, the RMSE values are relatively high over the Kuroshio extension and the region to the north, the Gulf Stream, the WWD and the Tropical Eastern Pacific region. The higher RMSE values for these regions are due in part to the strong mesoscale eddies there.

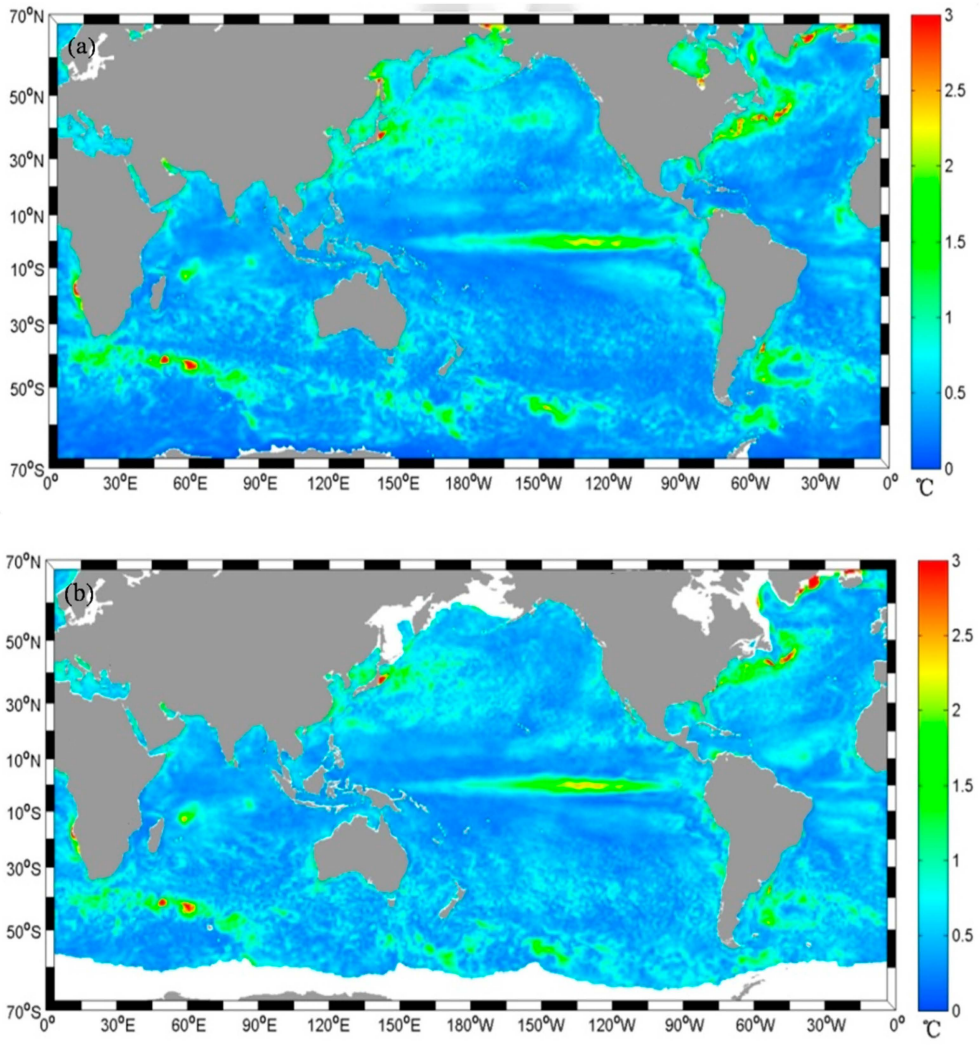

Figure 3. Distributions of global SST RMSE (°C) against the (**a**) OSTIA and (**b**) MGDSST.

3.2. Forecasting Error Statistics of SSH

The SSH is shown to be an important indicator of the upper ocean and is sensitive to the seawater density fluctuations [41]; thus, we shift the focus of analysis from the SST to SSH forecasting. The observations from the AVISO SSH are adopted to provide a reference to assess the performance of the dynamic characteristics in the upper ocean of NMEFC-MOM4. The monthly average difference in the SSH is carried out by subtracting observations from NMEFC-MOM4. Since the SSH difference has a similar spatial distribution from August to November 2013, Figure 4a shows the average SSH difference in August as a representative distribution. The SSH of NMEFC-MOM4 is well represented at the middle and low latitudes of the ocean where there are small negative values of model bias. Additionally, the positive values are basically located in the Kuroshio extension, the Gulf Stream and the region to the north of the Gulf Stream. It is clear that the positive and negative values are alternatively distributed in the Antarctic Circumpolar Current (ACC) region of the Southern Ocean.

We then calculate the standard deviation (STD) differences between the forecasting SSH from NMEFC-MOM4 and AVISO (Figure 4b). The positive STD differences are in the ACC region, which indicates that the SSH variability of NMEFC-MOM4 is stronger than that of the observation. There are mainly negative differences in most other regions, especially in the Kuroshio extension and Gulf Stream.

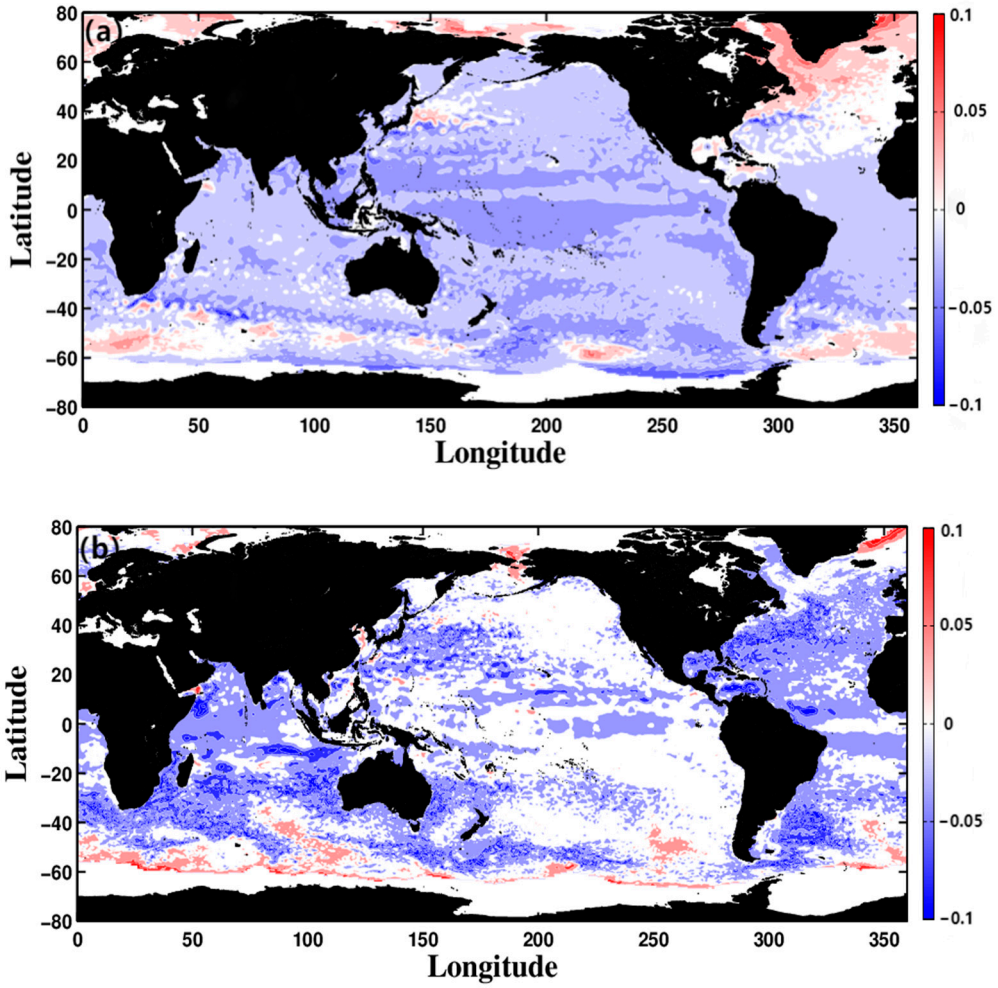

Figure 4. Distributions of global average SSH (**a**) bias and (**b**) STD differences between NMEFC-MOM4 and AVISO observations.

3.3. Forecasting Error Statistics of Temperature–Salinity Profiles

The temperature and salinity forecasting profiles are evaluated with GTS buoy observation datasets (Table 1). Six station locations from GTS FM18 and FM64 are selected with the corresponding observation data. The longitudes and latitudes of the GTS buoy locations are shown in Table 1. Our NMEFC-MOM4 24 h forecasting error statistics of the temperature profiles against the FM18 buoys are presented in Figure 5. Overall, the NMEFC-MOM4 24 h forecasting of the temperature vertical distribution is represented well compared to that of the GTS FM18 buoys observation. We also noticed a limitation of the forecasting temperature profile, characterized by the relatively shallower thermocline depth in comparison with the FM18 buoys observation. Regarding the salinity profiles' evaluation, a comparative analysis against the FM 64 buoys' observations is conducted to assess the performance of the NMEFC-MOM4 24 h forecasting products (Figure 6). The figure clearly shows that the salinity profiles forecasting from NMEFC-MOM4 correspond well with those of the GTS observation, except with a weaker cold bias between the depths of 100 and 200 m (about 0.2 PSU) at buoy station 2901494.

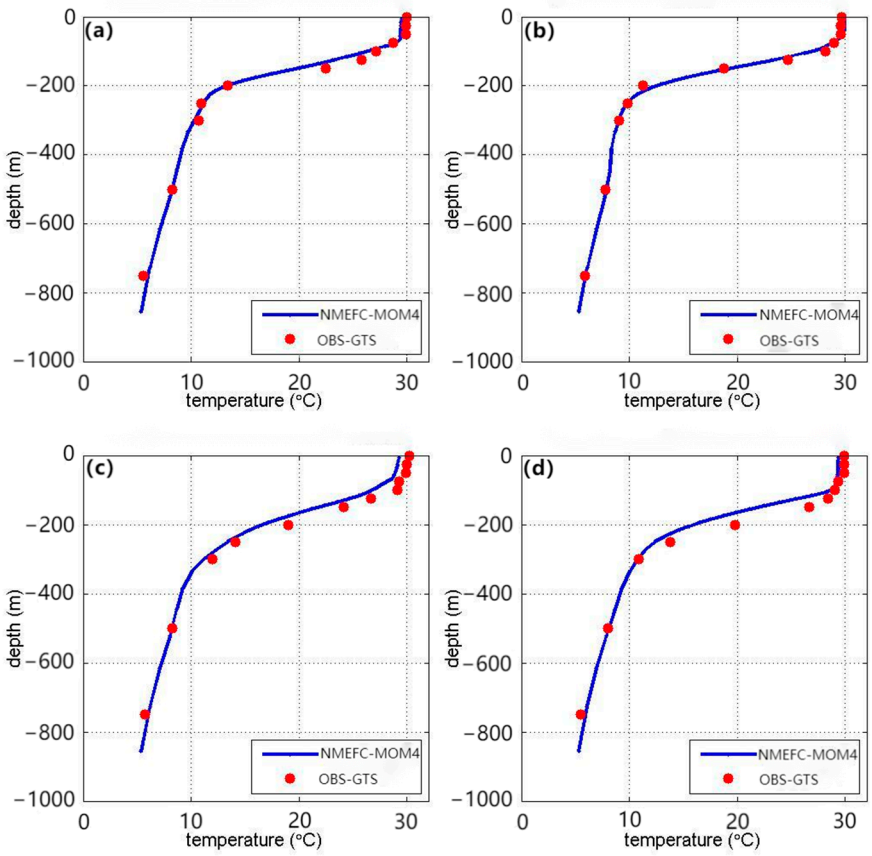

Figure 5. Vertical distribution of the NMEFC-MOM4 24 h forecasting temperature profiles (blue lines) compared with the observational GTS FM18 (red dots) on 1 August 2013 at buoy stations (**a**) 52,083, (**b**) 52,084, (**c**) 52,085 and (**d**) 52,088.

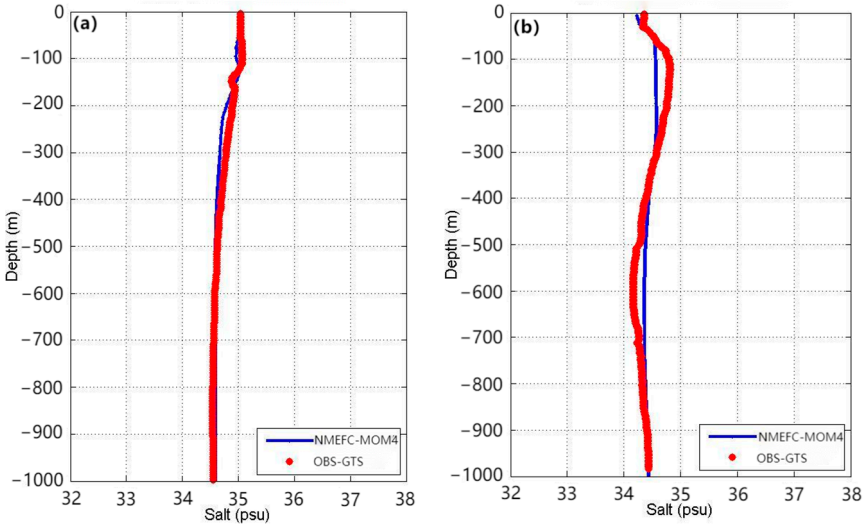

Figure 6. Vertical distribution of the NMEFC-MOM4 24 h forecasting salinity profiles (blue lines) compared with the observational GTS FM64 (red dots) at buoy station (**a**) 3,900,783 on 27 August 2013 and (**b**) station 2,901,494 on 26 August 2013.

Table 1. Longitudes and latitudes of the GTS buoys.

GTS	Station Number	Longitude (°E)	Latitude (°N)
FM18	52083	156.027	7.965
	52084	155.967	5.02
	52085	156.037	0.003
	52088	155.956	−2.019
FM64	3900783	219.757	−0.153
	2901494	126.229	21.505

4. Conclusions

In this study, we built a global-ocean-data-assimilation system based on the 3DVAR method and evaluated the assimilation effect for global-ocean analysis and forecasting products by comparing our results with those obtained with the OSTIA, MGDSST, AVISO and GTS buoys' observation datasets. The results of the comparative analysis are encouraging since they show that the 3DVAR assimilation method can effectively improve the simulation and forecasting performance by providing a better initial condition. Overall, the analysis SST of NMEFC-MOM4 agrees well with the OSTIA and MGDSST, with a respective averaged RMSE of 0.523 and 0.548 °C. The forecasting SSH of NMEFC-MOM4 is well represented at the middle and low latitudes, with a relatively large bias in the strong mesoscale eddies regions. As for the forecasting evaluation of the NMEFC-MOM4 T/S profiles, it has a good capability to capture the vertical distribution of temperature profiles when compared to that of the GTS buoys' observation. The salinity profiles forecasting from NMEFC-MOM4 correspond well with the GTS observation, except with a weaker cold bias between the depths of 100 and 200 m (about 0.2 PSU) at buoy station 2901494.

In summary, the 3DVAR assimilation method significantly improved the forecasting skill of operational oceanography. It should be noted that there was some limited improvement for the global-ocean surface environment in these regions with intense mesoscale activity and for temperature–salinity profiles in thermocline depths. Naturally, many continued efforts, such as increasing the model resolution, are continuously needed to improve the assimilation scheme and forecasting skills.

Author Contributions: Conceptualization, Y.Q. and L.W.; software, Q.Y.; validation, H.M., Y.W., S.M., D.S. and J.X.; formal analysis, Y.Q., Q.Y. and H.M.; investigation, Y.L.; resources, L.W. and X.W.; data curation, Q.Y. and H.M.; writing—original draft preparation, Y.Q.; writing—review and editing, Q.Y. and L.W.; visualization, H.M.; supervision, L.W.; project administration, X.W. and Y.L.; funding acquisition, L.W. and Y.Q. All authors have read and agreed to the published version of the manuscript.

Funding: This research was funded by the National Basic Research Program of China, grant number 2021YFC3101504, and the National Natural Science Foundation of China, grant number 42176030.

Institutional Review Board Statement: Not applicable.

Informed Consent Statement: Not applicable.

Data Availability Statement: The RTG SST was sourced from ftp://ftpprd.ncep.noaa.gov (accessed on 1 March 2013); the temperature-salinity profiles from Argo floats was obtained from the FTP site ftp://ftp.ifremer.fr/ifremer/argo (accessed on 27 February 2013); the OSTIA was available at https://marine.copernicus.eu/ (accessed on 2 August 2013).

Acknowledgments: We thank all the associated institutes or organizations for providing the remote sensing SST, sea-surface altimeter, Argo floats and GTS observations through the internet. Y.Q. (Yinghao Qin) wants to offer the most heartfelt thanks to his wife Lin Wang, the mother of Huhu and Tutu, who he loves more than anything in the world. He thanks her for her eternal love, encouragement and support.

Conflicts of Interest: The authors declare no conflict of interest.

References

1. Tippett, M.K. Extreme weather and climate. *npj Clim. Atmos. Sci.* **2018**, *1*, 45. [CrossRef]
2. Cummings, J.A. Operational multivariate ocean data assimilation. *Q. J. R. Meteorol. Soc.* **2005**, *131*, 3583–3604. [CrossRef]
3. Metzger, E.J.; Smedstad, O.M.; Thoppil, P.; Hurlburt, H.E.; Wallcraft, A.J.; Franklin, D.S.; Shriver, J.F.; Smedstad, L.F. Validation Test Report for the Global Ocean Prediction System V3.0—1/12° HYCOM/NCODA: Phase I. NRL Memorandum Report NRL/MR/7320—08-9148. 85p. Naval Research Laboratory, Oceanography Division, Stennis Space Center, Miss. Available online: http://www7320.nrlssc.navy.mil/pubs/2008/metzger-2008.pdf (accessed on 23 November 2023).
4. Metzger, E.J.; Smedstad, O.M.; Thoppil, P.; Hurlburt, H.E.; Franklin, D.S.; Peggion, G.; Shriver, J.F.; Townsend, T.L.; Wallcraft, A.J. Validation Test Report for the Global Ocean Forecast System V3.0— 1/12° HYCOM/NCODA: Phase II. NRL Memorandum Report NRL/MR/7320—10-9236. 76p. Naval Research Laboratory, Oceanography Division, Stennis Space Center, Miss. Available online: http://www7320.nrlssc.navy.mil/pubs/2010/metzger1-2010.pdf (accessed on 23 November 2023).
5. Me Metzger, E.J.; Smedstad, O.M.; Thoppil, P.; Hurlburt, H.E.; Cummings, J.A.; Wallcraft, A.J.; Zamudio, L.; Franklin, D.S.; Posey, P.G.; Phelps, M.W.; et al. US Navy operational global ocean and Arctic ice prediction systems. *Oceanography* **2014**, *27*, 32–43. [CrossRef]
6. Bell, M.J.; Lefèbvre, M.; Le Traon, P.Y.; Smith, N.; Wilmer-Becker, K. GODAE: The Global Ocean Data Assimilation Experiment. *Oceanography* **2009**, *22*, 14–21. [CrossRef]
7. Mogensen, K.S.; Balmaseda, M.A.; Weaver, A.; Martin, M.J.; Vidard, A. NEMOVAR: A variational data assimilation system for the NEMO ocean model. *ECMWF Newsl.* **2009**, *120*, 17–21. [CrossRef]
8. Mogensen, K.S.; Balmaseda, M.A.; Weaver, A. *The NEMOVAR Ocean Data Assimilation System as Implemented in the ECMWF Ocean Analysis for System 4*; ECMWF Technicam Memorandum 668; European Centre for Medium-Range Weather Forecasts: Reading, UK, 2012.
9. Blockley, E.W.; Martin, M.J.; McLaren, A.J.; Ryan, A.G.; Waters, J.; Lea, D.J.; Mirouze, I.; Peterson, K.A.; Sellar, A.; Storkey, D. Recent development of the Met Office operational ocean forecasting system: An overview and assessment of the new Global FOAM forecasts. *Geosci. Model Dev. Discuss.* **2013**, *6*, 6219–6278. [CrossRef]
10. Waters, J.; Lea, D.J.; Martin, M.J.; Storkey, D.; While, J. *Describing the Development of the New FOAM-NEMOVAR System in the Global 1/4 Degree Configuration*; Technical Report 578; Met Office: Exter, UK, 2013.
11. Waters, J.; Lea, D.J.; Martin, M.J.; Mirouze, I.; Weaver, A.T.; While, J. Implementing a variational data assimilation system in an operational 1/4 degree global ocean model. *Q. J. R. Meteorol. Soc.* **2014**, *141*, 333–334. [CrossRef]
12. Tranchant, B.; Testut, C.E.; Ferry, N.; Birol, F.; Brasseur, P. SAM2: The second generation of Mercator assimilation system. In Proceeding of the 4th International Conference on EUROGOOS, Brest, France, 6–9 June 2005.
13. Brasseur, P.; Bahurel, P.; Bertino, L.; Birol, F.; Brankart, J.M.; Ferry, N.; Losa, S.; Remy, E.; Schröter, J.; Skachko, S.; et al. Data assimilation in operational ocean forecasting systems: The MERCATOR and MERSEA developments. *Q. J. R. Meteorol. Soc.* **2005**, *22*, 3561–3582. [CrossRef]
14. Pham, D.; Verron, J.; Roubaud, M. A Singular Evolutive Extended Kalmanfilter for data assimilation in oceanography. *J. Mar. Syst.* **1998**, *16*, 323–340. [CrossRef]
15. Testut, C.E.; Brasseur, P.; Brankart, H.M.; Verron, J. Assimilation of seasurface temperature and altimetric observations during 1992–1993 into an eddy-permitting primitive equation model of the North Atlantic Ocean. *J. Mar. Syst.* **2003**, *40–41*, 291–316. [CrossRef]
16. Tranchant, B.; Testut, C.E.; Bourdallé-Badie, R.; Derval, C.; Le Galloudec, O.; Drillet, Y. The global 1/12°Mercator Ocean forecasting system: Scientific design and first results. In Proceedings of the GODAE Final Symposium, Nice, France, 12–15 November 2008.
17. Ferry, N.; Parent, L.; Garric, G.; Barnier, B.; Jourdain, N.C. The Mercator Ocean team: Mercator Global Eddy Permitting Ocean Reanalysis GLORYS1V1: Description and Results. *Mercat. Ocean. Q. Newsl.* **2010**, *36*, 15–27.
18. Lellouche, J.M.; Le Galloudec, O.; Drévillon, M.; Régnier, C.; Greiner, E.; Garric, G.; Ferry, N.; Desportes, C.; Testut, C.E.; Bricaud, C.; et al. Evaluation of Global Monitoring and Forecasting Systems at Mercator Océan. *Ocean Sci.* **2013**, *9*, 57–81. [CrossRef]
19. Griffies, S.M.; Harrison, M.J.; Pacanowski, R.C.; Rosati, A. *A Technical Guide to MOM4*; NOAA/Geophysical Fluid Dynamics Laboratory: Princeton, NJ, USA, 2003.
20. Tolman, H.L. *User Manual and System Documentation of WAVEWATCH III TM Version 3.14*; Technical Note 276; NOAA/NWS/NCEP/MMAB: Camp Springs, MD, USA, 2009; p. 194. Available online: https://polar.ncep.noaa.gov/mmab/papers/tn276/MMAB_276.pdf (accessed on 23 November 2023).
21. Chen, C.S.; Beardsley, R.C.; Cowles, G. *An Unstructured Grid, Finite-Volume Coastal Ocean Model: FVCOM User Manual*; SMAST/UMASSD: New Bedford, MA, USA, 2006.
22. Kleist, D.T.; Parrish, D.F.; Derber, J.C.; Treadon, R.; Errico, R.M.; Yang, R. Improving incremental balance in the GSI 3DVAR analysis system. *Mon. Weather. Rev.* **2009**, *137*, 1046–1060. [CrossRef]
23. Kleist, D.T.; Parrish, D.F.; Derber, J.C.; Treadon, R.; Wu, W.S.; Lord, S. Implementation of a new 3DVAR analysis as part of the NCEP global data assimilation system. *Weather Forecast.* **2008**, *24*, 1691–1705. [CrossRef]

24. Han, J.; Pan, H.L. Revision of convection and vertical diffusion schemes in the NCEP global forecast system. *Weather Forecast.* **2011**, *26*, 520–533. [CrossRef]
25. Greatbatch, R.J.; Lu, Y.; Cai, Y. Relaxing the Boussinesq approximation in ocean circulation models. *J. Atmos. Ocean. Technol.* **2001**, *18*, 1911–1923. [CrossRef]
26. Campin, J.-M.; Goosse, H. Parameterization of density-driven downsloping flow for a coarse-resolution ocean model in z-coordinate. *Tellus* **1999**, *51A*, 412–430. [CrossRef]
27. Gent, P.R.; McWilliams, J.C. Isopycnal mixing in ocean circulation models. *J. Phys. Oceanogr.* **1990**, *20*, 150–155. [CrossRef]
28. Griffies, S.M. The Gent-McWilliams skew-flux. *J. Phys. Oceanogr.* **1998**, *28*, 831–841. [CrossRef]
29. Large, W.G.; McWilliams, J.C.; Doney, S.C. Oceanic vertical mixing: A review and a model with a nonlocal boundary layer parameterization. *Rev. Geophys.* **1994**, *32*, 363–403. [CrossRef]
30. Li, Z.; McWilliams, J.C.; Ide, K.; Farrara, J.D. A multiscale variational data assimilation scheme: Formulation and illustration. *Mon. Weather. Rev.* **2015**, *143*, 3804–3822. [CrossRef]
31. Wang, D.X.; Qin, Y.H.; Xiao, X.J.; Zhang, Z.Q.; Wu, F.M. Preliminary results of a new global ocean reanalysis. *Chin. Sci. Bull.* **2012**, *57*, 3509–3517. [CrossRef]
32. De Vos, M.; Backeberg, B.; Counillon, F. Using an eddy-tracking algorithm to understand the impact of assimilating altimetry data on the eddy characteristics of the agulhas system. *Ocean. Dyn.* **2018**, *68*, 1071–1091. [CrossRef]
33. Martin, M.J.; Balmaseda, M.; Bertino, L.; Brasseur, P.; Brassington, G.; Cummings, J.; Fujii, Y.; Lea, D.J.; Lellouche, J.M.; Mogensen, K.; et al. Status and future of data assimilation in operational oceanography. *J. Oper. Oceanogr.* **2015**, *8* (Suppl. 1), s28–s48. [CrossRef]
34. Tonani, M.; Balmaseda, M.; Bertino, L.; Blockley, E.; Brassington, G.; Davidson, F.; Drillet, Y.; Hogan, P.; Kuragano, T.; Lee, T.; et al. Status and future of global and regional ocean prediction systems. *J. Oper. Oceanogr.* **2015**, *8* (Suppl. 2), s201–s220. [CrossRef]
35. Da Rocha Fragoso, M.; de Carvalho, G.V.; Soares, F.L.M.; Faller, D.G.; de Freitas Assad, L.P.; Toste, R.; Sancho, L.M.B.; Passos, E.N.; Böck, C.S.; Reis, B.; et al. A 4D-variational ocean data assimilation application for Santos Basin, Brazil. *Ocean. Dyn.* **2016**, *66*, 419. [CrossRef]
36. Donlon, C.J.; Martin, M.; Stark, J.D.; Roberts-Jones, J.; Fiedler, E.; Wimmer, W. The Operational Sea Surface Temperature and Sea Ice analysis (OSTIA). *Remote Sens. Environ.* **2012**, *116*, 140–158. [CrossRef]
37. Sakurai, T.; Yukio, K.; Kuragano, T. Merged satellite and insitu data global daily SST. In Proceedings of the 2005 IEEE International Geoscience and Remote Sensing Symposium, Seoul, Republic of Korea, 29 July 2005; pp. 2606–2608.
38. Zuidema, P.; Chang, P.; Medeiros, B.; Kirtman, B.P.; Mechoso, R.; Schneider, E.K.; Toniazzo, T.; Richter, I.; Small, R.J.; Bellomo, K.; et al. Challenges and prospects for reducing coupled climate model SST biases in the eastern tropical Atlantic and Pacific oceans: The US CLIVAR Eastern Tropical Oceans Synthesis Working Group. *Bull. Am. Meteorol. Soc.* **2016**, *97*, 2305–2328. [CrossRef]
39. McClean, J.L.; Bader, D.C.; Bryan, F.O.; Maltrud, M.E.; Dennis, J.M.; Mirin, A.A.; Jones, P.W.; Kim, Y.Y.; Ivanova, D.P.; Vertenstein, M.; et al. A prototype two-decade fully-coupled fine-resolution CCSM simulation. *Ocean Modell.* **2011**, *39*, 10–30. [CrossRef]
40. Delworth, T.L.; Rosati, A.; Anderson, W.; Adcroft, A.J.; Balaji, V.; Benson, R.; Dixon, K.; Griffies, S.M.; Lee, H.-C.; Pacanowski, R.C.; et al. Simulated climate change in the GFDL CM2.5 high-resolution coupled climate model. *J. Clim.* **2012**, *25*, 2755–2781. [CrossRef]
41. Zhuang, W.; Xie, S.P.; Wang, D.X.; Taguchi, B.; Aiki, H.; Sasaki, H. Intraseasonal variability in sea surfaceheight over the South China Sea. *J. Geophys. Res.* **2010**, *115*, C04010. [CrossRef]